

# Dynamics of helical-wave emission in a fiber-coupled diode end-pumped solid-state laser

Y.F. Chen<sup>1,\*</sup>, Y.P. Lan<sup>2</sup>

<sup>1</sup> Department of Electrophysics, National Chiao Tung University, 1001 TA Hsueh Road, Hsinchu 30050, Taiwan, Republic of China

<sup>2</sup> Institute of Electro-Optical Engineering, National Chiao Tung University Hsinchu, Taiwan, Republic of China

Received: 14 November 2000/Revised version: 22 January 2001/Published online: 23 May 2001 – © Springer-Verlag 2001

**Abstract.** We have generated  $TEM_{0,l}^*$  modes in an end-pumped microchip laser using a standard fiber-coupled diode. A rich set of dynamic behaviors, such as periodic and quasi-periodic self-modulation, chaotic pulsing and frequency locking was observed in the generated  $TEM_{0,l}^*$  modes. Experimental results confirm the theoretical predictions that the locking occurs as a subcritical bifurcation and that a region of coexisting locked and unlocked states exists.

**PACS:** 42.55.Rz; 42.60.Mi; 42.65.Sf

Optical vortices in lasers have been observed in low-order transverse modes containing one or several phase singularities [1–4]. The simplest examples are Laguerre-Gaussian fields  $TEM_{p,l}^*$  with  $p = 0$ , the doughnut modes of charge  $l$ , which consist of  $l$  helical wave fronts winding about each other, around the cavity axis. Here  $p$  and  $l$  are the radial and azimuthal indices of the LG mode. These have circularly symmetric doughnut-shaped intensity distributions. In recent years the mechanical and optical effects of  $TEM_{0,l}^*$  modes have attracted a great deal of interest because they possess well-defined angular momentum along the optical axis when  $l$  is not zero [5]. These modes are also important in laser cooling and trapping experiments [6]. Therefore, study of the generation of LG  $TEM_{0,l}^*$  modes in solid-state lasers is of great interest.

Recently, we reported a technique for the generation of cylindrically symmetric LG modes with  $p = 0$ , and specified values of  $l$  in a fiber-coupled diode end-pumped solid-state laser [7]. The key novelty was to produce a doughnut-shaped pump-profile by defocusing a standard fiber-coupled diode. Experimental results demonstrate that the stable transverse-mode pattern near the pump threshold is usually a LG  $TEM_{0,l}$  mode with the distribution  $\cos^2 l\theta$  (or  $\sin^2 l\theta$ ) in the azimuthal angle, having  $2l$  nodes in azimuth. Even though the geometry is of cylindrical symmetry, there is still a certain astigmatism in the cavity due to the thermal lensing effect and anisotropic properties of the gain medium. This is the reason why sine

or cosine LG modes were generated near the pump threshold, instead of doughnut modes. A similar high-order LG  $TEM_{0,l}$  mode has been reported in electrically pumped [8] and optically pumped [9] vertical-cavity surface-emitting semiconductor lasers (VCSELs). However, the main difficulty associated with the emission of high-order LG modes in VCSELs is that the processed wafer needs to be of extraordinary homogeneity.

Slightly above the pump threshold, a LG  $TEM_{0,l}^*$  or  $TEM_{0,-l}^*$  mode, having a circle of constant intensity in the radial direction, can be generated by the superposition of two like  $TEM_{0,l}$  modes, which have a fixed relative phase equal to  $\pi/2$ . Astigmatism-induced splitting of the like mode frequencies has a significant influence on laser dynamics. Temporal instabilities and chaotic emission caused by the non-linear interaction of transverse modes in a class-A laser have been reported by Tamm [10], who experimentally confirmed the existence of a “cooperative frequency locking” state [11] for the nearly degenerate  $TEM_{0,1}$  and  $TEM_{1,0}$  modes of a helium-neon laser. However, the dynamic characteristics of a solid-state laser are those of an oscillator with an inertial (non-instantaneous) non-linearity. In the case of such oscillators, the perturbations exhibit oscillatory relaxation. Because of relaxation oscillations, the two-mode locking in a class-B laser occurs as a subcritical bifurcation [12, 13], unlike that in class-A lasers where the locking is a supercritical bifurcation. Recently, Zehnlé [14] analytically studied the dynamic behavior of class A and B lasers operating in two transverse modes. His analysis provides evidence of the qualitative differences in the stationary as well as periodic behaviors for class A and B bimodal lasers. Even so, to date not much has been done to observe these differences.

In this work, we perform an experimental investigation of the relaxation oscillations in a solid-state laser with helical wave emission. Experimental results show that the relaxation oscillations play an important role not only in locking processes, but also under stationary state conditions. A rich set of dynamic behaviors, such as periodic and quasi-periodic self-modulation, chaotic pulsing, and frequency locking was observed experimentally in the generated  $TEM_{0,l}^*$  hybrid mode. It was found that the experimental data exhibited a generally satisfactory agreement with the theoretical predictions.

\*Corresponding author.

(Fax: +886-35/729-134, E-mail: yfchen@cc.nctu.edu.tw)

## 1 Results and discussion

A non-linear system of the Maxwell–Bloch equations, given in terms of partial derivatives, is usually reduced to a system of ordinary differential equations by expanding in terms of the empty-cavity modes for the laser system with a small number of excited transverse modes [12–16]. The dynamics of generating two transverse modes in a class-B laser was investigated theoretically [12, 13]. The main results of the calculations can be summarized as follows.

When the frequency difference between two like  $TEM_{0,l}$  modes,  $\Delta\Omega$  is greater than the relaxation frequency  $\omega_r$ , the total intensity exhibits a self-modulation oscillation. The self-modulation oscillation can be periodic or quasi-periodic, depending on the magnitude of the frequency difference  $\Delta\Omega$ . When  $\Delta\Omega \gg \omega_r$  the total intensity in the self-modulation regime is a periodic oscillation. However, when  $\Delta\Omega$  is close to the relaxation frequency in the self-modulation regimes, the total intensity is like to a quasi-periodic oscillation. In addition to the self-modulation regimes characterized by periodic or quasi-periodic modulation, dynamic chaos can appear under the conditions of  $\omega_r/2 < \Delta\Omega < \omega_r$ . Note that the system of equations for the dynamics of a class B laser operating in two LG modes with opposite angular indices  $\pm l$  is like to the system describing the generation of a counter-propagating wave (CPW) in a bidirectional ring class-B laser, as discussed in [17–19]. Therefore, the condition for chaotic emission is also predicted in a bidirectional ring class-B laser [18]. When  $\Delta\Omega < \omega_r/2$ , the intensity represents the frequency-locked transverse mode. In class-B lasers the locking occurs at a significantly smaller mode frequency difference,  $\Delta\Omega < \omega_r/2$ . Thus it is more difficult to obtain frequency locking in class-B than in class-A lasers. The relaxation oscillation plays an important role, not only in transient processes but also under conditions of steady operation of a solid-state laser (class-B laser). The build-up of the relaxation oscillation is one of the mechanisms resulting in the appearance of dynamic chaos in solid-state lasers. Using the system of equations given in [13], we find that if the loss difference is introduced near the locking region in a class B laser, the total intensity may exhibit a self-pulsing train. The total intensity under the self-pulsing region is almost like a LG  $TEM_{0,l}$  mode with the distribution  $\cos^2 l\theta$  (or  $\sin^2 l\theta$ ) in azimuthal angle because of loss difference. The self-pulsing phenomenon is like to the recent result concerning the dynamics of a solid-state laser sustaining the oscillation of two orthogonally-polarized eigenstates [20].

Figure 1 shows the schematic diagram of the fiber-coupled laser diode end-pumped Nd:YVO<sub>4</sub> laser considered in this work. We used a plano-concave cavity that consisted of one planar Nd:YVO<sub>4</sub> surface (high-reflection-coated at 1064 nm and high-transmission-coated at 809 nm) for the pump light to enter the laser crystal, and a spherical output mirror. The second surface of the Nd:YVO<sub>4</sub> crystal (1 mm in length) was anti-reflection coated at 1064 nm. A mirror with a reflectance of  $R = 97\%$  and a radius of curvature of 25 cm was used in the resonator to couple the output power. For a 1 cm resonator length, the waist of the fundamental mode was around 0.24 mm. The fiber-coupled laser diode (Coherent, F-81-800C-100) had a core diameter of 0.1 mm and was focused into the Nd:YVO<sub>4</sub> crystal using a focusing lens with a magnification of 0.57.

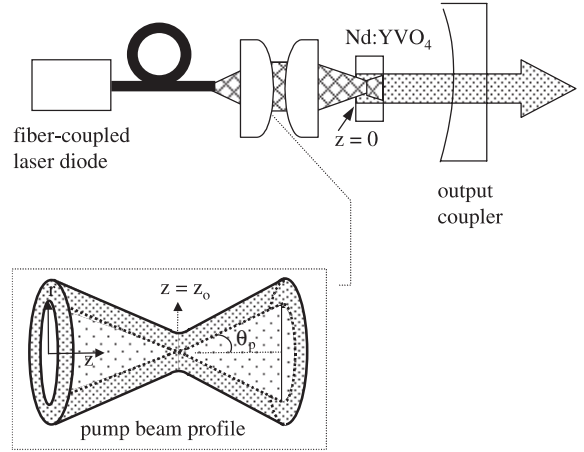


**Fig. 1.** Schematic diagram of a fiber-coupled diode end-pumped laser; a typical beam profile of a fiber-coupled laser diode away from the focal plane

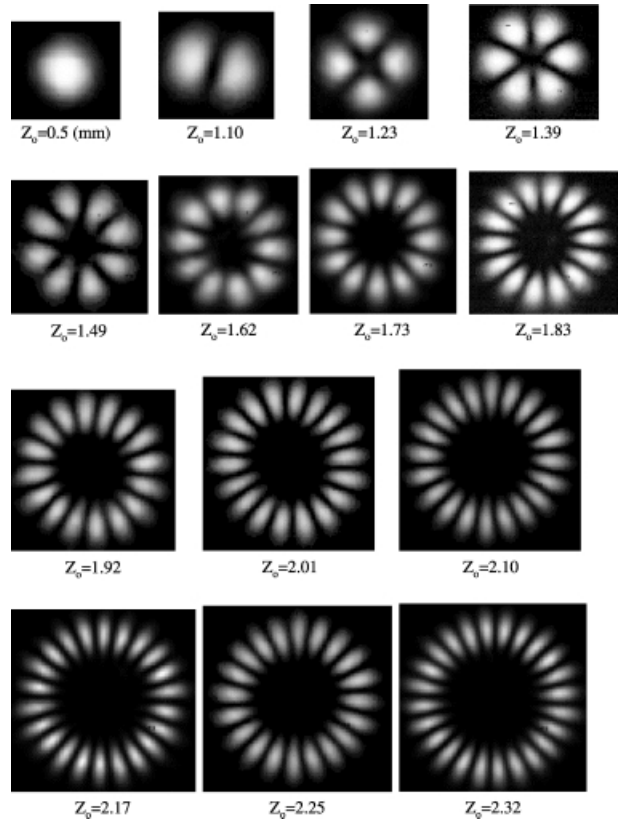


**Fig. 2.** Beam profiles with different LG  $TEM_{0,l}$  mode distributions, measured with the CCD camera, in 14 positions

For the beam of a multi-mode fiber-coupled diode laser passing through a focusing lens, the profile at the focal plane is like a top hat-shaped distribution; however, away from the focal plane it is like a doughnut-shaped distribution, as depicted in Fig. 1. With this property, we can defocus a standard fiber-coupled diode beam, resulting in a good overlap with the high-order LG  $TEM_{0,l}$ -mode and generate it purely. From the characteristics of the pump beam profile, the radius of maximum pump intensity amplitude can be approximately described by  $r_p(z) = \theta_p |z - z_0|$ , where  $\theta_p$  is the far-field half-

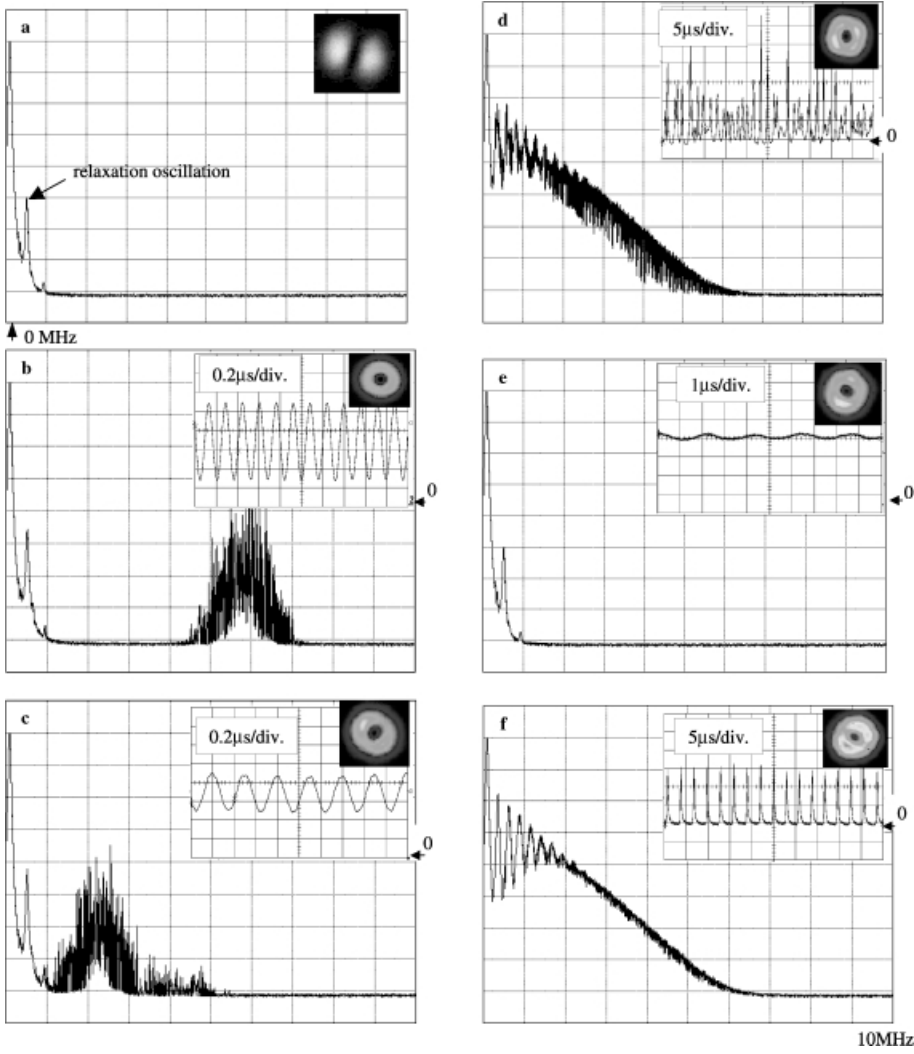


**Fig. 3.** a Power intensity spectra of laser emission for one  $\text{TEM}_{0,l}^*$  mode. Spectra b–f are recorded when the laser simultaneously oscillates in the two first-order transverse modes, showing the transition from the self-modulation state (b) and (c) to chaotic pulsing (d) and the frequency-locked state (e), and the bifurcation of the locking to regular self-pulsing (f). Vertical scale: 10 dB/div; horizontal scale: 1 MHz/div. Average transverse intensity distribution and time dependence are shown in the insets

angle, the point  $z = 0$  is taken to be at the incident surface of the gain medium and  $z_0$  is the focal position of the pump beam in the laser crystal. The average radius of maximum pump intensity inside the gain medium,  $r_{\text{pa}}$ , is calculated by  $\int_0^L r_p(z) e^{-\alpha z} dz / \int_0^L e^{-\alpha z} dz$ , where  $\alpha$  is the absorption coefficient at the pump wavelength and  $L$  is the length of the laser crystal. Carrying out the integration and using  $e^{-\alpha L} \rightarrow 0$ , the average radius of maximum pump intensity is given by  $r_{\text{pa}} = \theta_p [z_0 + (2e^{-\alpha z_0} - 1)/\alpha]$ .

For a single LG  $\text{TEM}_{0,l}$  mode, the normalized cavity mode distribution is given by

$$s_{0,l}(r, \phi, z) = \frac{4}{(1 + \delta_{0,l})!} \frac{1}{\pi \omega_0^2 L} (\cos^2 l\phi) \left( \frac{2r^2}{\omega_0^2} \right)^l \times \exp\left(-\frac{2r^2}{\omega_0^2}\right), \quad (1)$$

where the  $z$ -dependent variation in  $s_{0,l}(r, \phi, z)$  is neglected and the spot radius of the laser beam  $\omega_0$  is approximated to be constant along the laser axis in the laser crystal. From (1), the radius of maximum mode intensity amplitude is trivially  $r_{0,l} = \omega_0 \sqrt{l/2}$ . Since the cavity mode with the biggest overlap with the gain structure has the minimum threshold, we

can obtain a LG  $\text{TEM}_{0,l}$ -mode output by adjusting the focal position  $z_0$  to achieve  $r_{\text{pa}} = r_{0,l}$  for the best overlap. Figure 2 shows the experimental results for the output beam profiles with different transverse-mode distributions, measured with a CCD camera (Coherent, Beam-Code), in fourteen positions. The relation between transverse-modes and pump positions is consistent with the prediction of pump-to-mode matching.

Typically, the free-running one-mode class-B laser displays relaxation oscillations, as shown in Fig. 3a. Relaxation oscillations play an important role in the locking of two-mode class-B lasers. With a pump power slightly larger than the pump threshold, the laser is operated in LG  $\text{TEM}_{0,l}^*$  doughnut mode, which is a linear combination of two like  $\text{TEM}_{0,l}$  modes that have a fixed relative phase equal to  $\pi/2$ . Since astigmatism lifts the degeneracy of the two like LG  $\text{TEM}_{0,l}$  modes, a perfectly circular pattern is usually an “unlocked doughnut” as can be confirmed by the observation of a periodic oscillation shown in Fig. 3b. From the state of the perfectly circular pattern, the frequency difference between the two nearly-degenerate modes can be decreased by a slight adjustment in the output coupler to result in quasi-periodic oscillation, as shown in Fig. 3c. It is found that the experimental results in the self-modulation regimes are consistent with theoretical predictions. Upon further decreasing the frequency

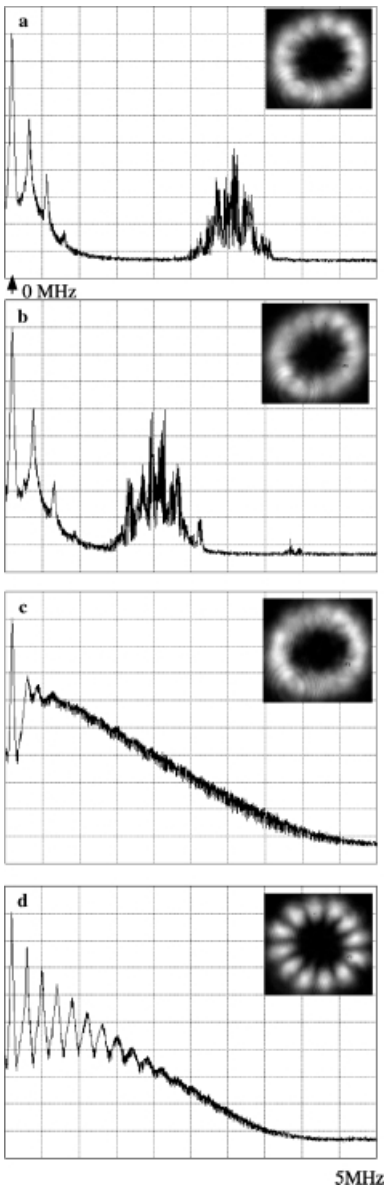


**Fig. 4a–d.** Power intensity spectra of laser emission for  $TEM_{0,6}^*$  mode. Spectra **a–d** show the transition from the self-modulation state (**a**) and (**b**) to chaotic pulsing (**c**), and the bifurcation of the locking to regular self-pulsing (**d**). Vertical scale: 10 dB/div; horizontal scale: 0.5 MHz/div

difference, the appearance of chaotic generation regimes was observed, as shown in Fig. 3d. This result confirms the fact that there is a chaotic set of solutions when the frequency difference is of the order of magnitude of the relaxation frequency. Upon decreasing the frequency difference below the locking threshold, the two like modes eventually lock to the same frequency, as shown in Fig. 3e. We observed that the locking state has a strong tendency to jump to states of chaotic pulsing if subjected to a small perturbation. The bistable region of coexistence between locked and unlocked modes was observed, which confirms the fact that the locking in a class-B laser is a subcritical bifurcation, as opposed to that in a class-A laser [12]. In the vicinity of the locking point, slightly adjusting the output coupler frequently may lead to very stable, regular self-pulsing operation of the laser, as shown in Fig. 3f. Note that there are two obvious intensity maxima superposed

on the background of the doughnut intensity distribution in the self-pulsing operation. We found that the regular self-pulsing state can hold for several hours, like a passively Q-switched laser. In addition, it is striking to notice that the repetition rate of the self-pulsing is slightly below the relaxation oscillation frequency. Moreover, we experimentally observed that the repetition rate increases with the pumping rate of the laser. The self-pulsed regime is experimentally obtained only in the vicinity of the locking point. This result proves that this self-pulsed regime is due to both the frequency locking of the two nearly-degenerate modes and the existence of relaxation oscillations, i.e., to the fact that the population inversion cannot be eliminated adiabatically in class-B lasers [12, 13]. Finally, we also found a dynamic-like behavior similar to a  $TEM_{0,1}^*$  mode for other higher  $TEM_{0,l}^*$  modes, i.e. periodic and quasi-periodic self-modulation (Fig. 4a and b), chaotic pulsing (Fig. 4c), and self-pulsing (Fig. 4d).

## 2 Summary

We have generated the LG  $TEM_{0,l}$  and  $TEM_{0,l}^*$  modes in an end-pumped microchip laser by defocusing a standard fiber-coupled diode to produce a doughnut-shaped pump profile. From the observations of the locking phenomena of the first order family, it was found that the locking occurs as a subcritical bifurcation and a region of coexisting locked and unlocked states exists. These observations are consistent with the interesting theoretical predictions for class-B lasers. We believe that our experimental method gives a convenient way of furthering the investigation of the non-linear dynamics of LG  $TEM_{0,l}^*$  modes.

## References

1. M. Brambilla, F. Battipede, L.A. Lugiato, V. Penna, F. Prati, C. Tamm, C.O. Weiss: *Phys. Rev. A* **43**, 5090 (1991)
2. M. Harris, C.A. Hill, J.M. Vaughan: *Opt. Commun.* **106**, 161 (1994)
3. G. D'Alessandro, G.L. Oppo: *Opt. Commun.* **96**, 123 (1993)
4. G. Slekys, C.O. Weiss, D.Y. Tang, M.F.H. Tarroja: *J. Opt. Soc. Am. B* **11**, 2089 (1994)
5. L. Allen, M.W. Beijersbergen, R.J.C. Spreeuw, J.P. Woerdman: *Phys. Rev. A* **45**, 8185 (1992)
6. J.W. Tabosa, D.V. Petrov: *Phys. Rev. Lett.* **83**, 4967 (1999)
7. Y.F. Chen, Y.P. Lan, S.C. Wang: *Appl. Phys. B* **72**, 167 (2001)
8. Q. Deng, H. Deng, D.G. Deppe: *Opt. Lett.* **22**, 463 (1997)
9. S.F. Pereira, M.B. Willemsen, M.P. Van Exter, J.P. Woerdman: *Appl. Phys. Lett.* **73**, 2239 (1998)
10. C. Tamm: *Phys. Rev. A* **38**, 3960 (1988)
11. L.A. Lugiato, C. Oldano, L.M. Narducci: *J. Opt. Soc. Am. B* **5**, 879 (1988)
12. K. Staliunas, M.F.H. Tarroja, C.O. Weiss: *Opt. Commun.* **102**, 69 (1993)
13. D.V. Skryabin, A.G. Vladimirov, A.M. Radin: *Quantum Electronics QE-27*, 892 (1997)
14. V. Zehnlé: *Phys. Rev. A* **57**, 629 (1998)
15. M. Brambilla, M. Cattaneo, L.A. Lugiato, R. Pirovano, F. Prati, A.J. Kent, G.L. Oppo, A.B. Coates, C.O. Weiss, C. Green, E.J. D'Angelo, J.R. Tredicce: *Phys. Rev. A* **49**, 1427 (1994)
16. F. Prati, L. Zucchetti, G. Molteni: *Phys. Rev. A* **51**, 4093 (1995)
17. P.A. Khandokhin, Y.I. Khanin: *J. Opt. Soc. Am. B* **2**, 225 (1985)
18. N.V. Kravtsov, E.G. Lariontsev: *Quantum Electronics QE-24*, 841 (1994)
19. A.G. Vladimirov: *Optics Comm.* **149**, 67 (1998)
20. M. Brunel, O. Emile, M. Alouini, A.L. Floch, F. Bretenaker: *Phys. Rev. A* **59**, 831 (1999)